INTERNAL MEDICINE

□ CASE REPORT □

Surgically Cured, Relapsed Pneumococcal Meningitis Due to Bone Defects, Non-invasively Identified by Three-dimensional Multi-detector Computed Tomography

Takayoshi Akimoto[1], Akihiko Morita[1], Keiji Shiobara[1], Makoto Hara[1], Masayuki Minami[1], Katsunori Shijo[2], Yasuyuki Nomura[3], Shuntaro Shigihara[3], Hiroki Haradome[4], Osamu Abe[4] and Satoshi Kamei[1]

Abstract

A 43-year-old Japanese man presented with a history of bacterial meningitis (BM). He was admitted to our department with a one-day history of headache and was diagnosed with relapse of BM based on the cerebrospinal fluid findings. The conventional imaging studies showed serial findings suggesting left otitis media, a temporal cephalocele, and meningitis. Three-dimensional multi-detector computed tomography (3D-MDCT) showed left petrous bone defects caused by the otitis media, and curative surgical treatment was performed. Skull bone structural abnormalities should be considered a cause of relapsed BM. 3D-MDCT was useful for revealing the causal minimal bone abnormality and performing pre-surgical mapping.

Key words: pneumococcal meningitis, relapsed bacterial meningitis, bone defect, three-dimensional computed tomography (3D-CT), volume rendering CT, cephalocele

(Intern Med 55: 3665-3669, 2016)
(DOI: 10.2169/internalmedicine.55.7299)

Introduction

Bacterial meningitis (BM) is a neurological emergency. Early and appropriate antibiotic therapy improves the prognosis, but some patients with BM develop recurrence or relapse. The causes of recurrence or relapse are the spread of inflammation from neighboring organs, abscess formation, thrombosis, immunodeficiency, and anatomical abnormalities (1). Computed tomography (CT) and magnetic resonance imaging (MRI) are usually used to investigate the origin of the focus, abscess, and thrombosis. Brain three-dimensional (3D) multi-detector CT (MDCT) imaging is particularly useful for investigating precise bone structural abnormalities in the auditory ossicles or skull base (2). We herein describe a surgically cured case of relapsed pneumococcal BM related to temporal bone defects. In the present case, 3D-MDCT revealed the key features of the causal minimal bone abnormality, which led to successful surgical treatment.

Case Report

A 43-year-old Japanese man was transported by ambulance to an emergency hospital. At the examination, he was comatose with a temperature of 39.7℃. His left tympanic membrane was red, although tympanic membrane maceration and perforation and cerebrospinal fluid (CSF) rhinorrhea were not observed. The laboratory data showed a high white blood cell count (46,300 cells/μL) and C-reactive protein level (12.04 mg/dL). Lumbar puncture was performed. The results were as follows: CSF white cell count (WCC) 11,643 cells/μL (99% polymorphonuclear cells); total protein 762 mg/dL; glucose 40 mg/dL (serum glucose 237 mg/

[1]Division of Neurology, Department of Medicine, Nihon University School of Medicine, Japan, [2]Department of Neurological Surgery, Nihon University School of Medicine, Japan, [3]Department of Otolaryngology-Head and Neck Surgery, Nihon University School of Medicine, Japan and [4]Department of Radiology, Nihon University School of Medicine, Japan
Received for publication February 19, 2016; Accepted for publication April 26, 2016
Correspondence to Dr. Akihiko Morita, morita.akihiko@nihon-u.ac.jp

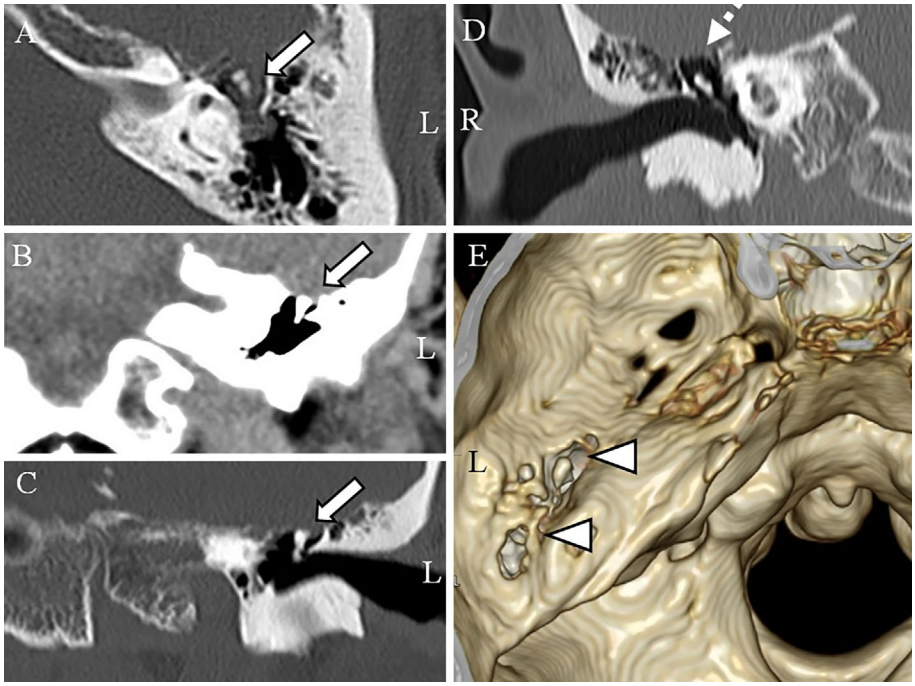

Figure 1. **A, B, C: The left temporal bone CT images (A axial view; B, C multi-planar reconstruction coronal view) show soft-tissue density at the left epitympanum and a partial defect of the left tegmen part of the petrous bone near the lesion (white arrows). D: A right temporal bone CT image of the multi-planar reconstruction coronal view shows thinning of the right tegmen tympani (white-striped arrow). E: A three-dimensional volume-rendering CT image (looking down on the skull base from above; Ziostation, Ziosoft, Tokyo, Japan) depicts 2 bone defects sized 12×9 mm and 9×5 mm at the tegmen tympani part of the left petrous bone (white arrowheads).**

dL); and Gram-positive cocci on Gram's stain. Ceftriaxone (CTRX) and linezolid (LZD) were administered intravenously. The CSF culture grew penicillin-resistant *Streptococcus pneumoniae* (minimum inhibitory concentration of benzyl penicillin was 1 μg/mL). On Day 7, the CSF WCC decreased to 49 cells/μL. On Day 14, CTRX and LZD were discontinued, and he was discharged on Day 22 without sequelae.

However, 11 days after being discharged from the emergency hospital, he was admitted to our department with a one-day history of headache and vomiting. On admission, he was conscious, with a temperature of 37.9℃, blood pressure of 137/89 mmHg, pulse of 98 beats per minute, and oxygen saturation of 100% on ambient air. The pupils were 4.0 mm in diameter and briskly reactive to light. The neck was not stiff. Neither deafness nor otorrhea was present. The findings from the remainder of the examination were normal. Chest radiographs and an electrocardiogram were negative. The temporal bone CT images showed soft-tissue density that invaded to the left tympanum and right tegmen tympani thinning (Fig. 1A-D). The pneumatization of the left mastoid cells was also decreased on the CT image. A 3D volume rendering CT (3D-CT) image (Ziostation; Ziosoft, Tokyo, Japan) revealed 2 petrous bone defects of 12×9 mm and 9×5 mm in size (Fig. 1E). Plain MRI showed spotty high-intensity areas along the cerebral falx on diffusion-weighted imaging (Fig. 2A). The left mastoid cells and middle ear showed a high-intensity area on T2-weighted imaging and a faint high-intensity area on diffusion-weighted imaging due to the T2 shine-through effect of mastoiditis (Fig. 2B and C). Contrast-enhanced T1-weighted images showed a minimal sac-like left temporal lobe protrusion into the petrous bone defect, suggesting a cephalocele (Fig. 2D-F). The laboratory data showed the following: white blood cell count 13,500/mm^3, with 88% neutrophils; C-reactive protein 0.79 mg/dL; creatinine 1.53 mg/dL; HbA1c 6.5%; and D-dimer <1.0 μg/mL. Two sets of blood cultures were sterile. Lumbar puncture was performed, and the results showed: CSF WCC 119 cells/μL (37% polymorphonuclear cells); total protein 78 mg/dL; and glucose 47 mg/dL (serum glucose 110 mg/dL). A CSF pneumococcal antigen test and CSF cultures of bacteria and acid-fast bacteria were negative.

The patient was diagnosed with relapsed BM with left mastoiditis. He was given intravenous meropenem (2 g every 8 hours), vancomycin (1 g every 12 hours), and dexamethasone (3.3 mg every 8 hours). His fever and headache were improved the next day. The CSF WCC decreased to 15 cells/μL on Day 6. However, on Day 24, he developed a whole-body rash, suggesting a drug eruption. The meropenem and vancomycin were changed to CTRX (2 g every 12 hours), LZD (600 mg every 12 hours), and oral rifampicin (600 mg every 24 hours). The drug-induced lymphocyte stimulation test was positive for both meropenem and

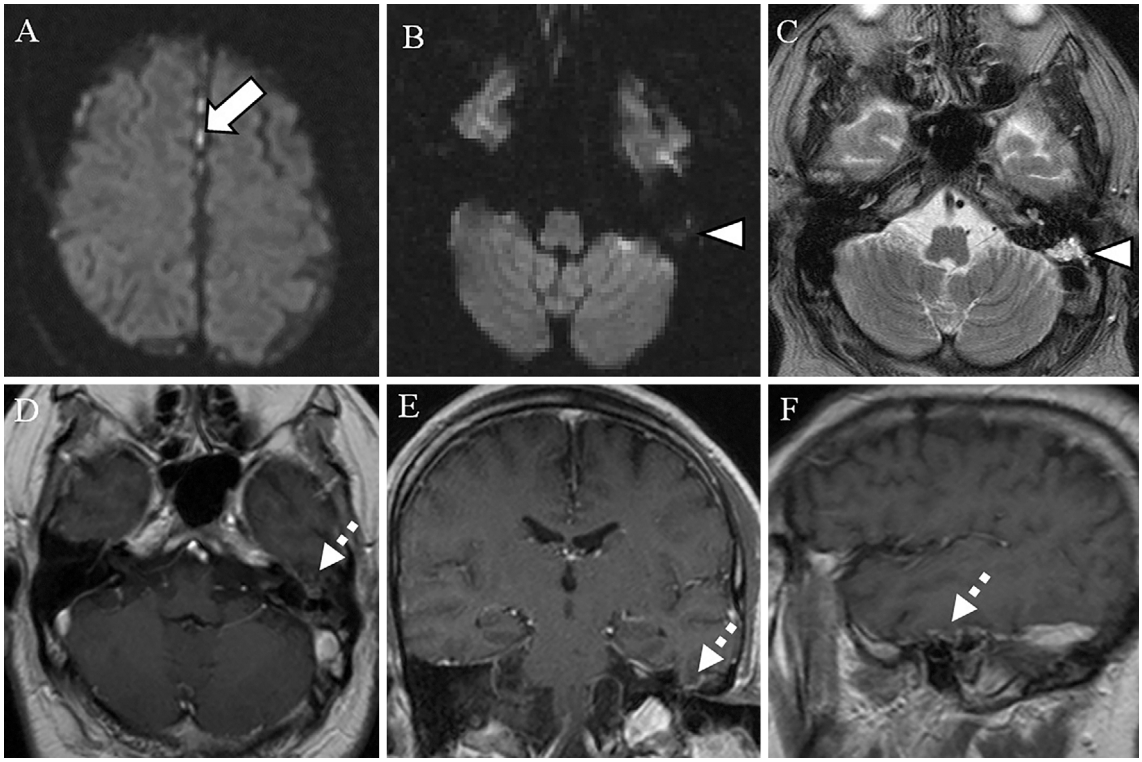

Figure 2. **A: An axial diffusion-weighted image shows several spotty, high-intensity areas along with the cerebral falx, suggesting meningitis-related purulent material (white arrow). B, C: An axial diffusion-weighted image shows a faint high-intensity area, probably due to the T2 shine-through effect of mastoiditis, at the left mastoid cells, but no intense signal (restricted diffusion) suggesting cholesteatoma. An axial T2-weighted image reveals a high-intensity area at the left middle ear corresponding to otitis media (white arrowheads). D, E, F: The axial, coronal, and sagittal contrast-enhanced T1-weighted images show a minimal sac-like left temporal lobe protrusion into the petrous bone defect, suggesting a cephalocele (white-striped arrows).**

vancomycin. On Day 38, his body temperature increased to 38.0℃, and his CSF WCC increased to 21 cells/μL. Furthermore, the pneumococcal antigen was detected in the CSF for the first time. On Day 49, Although the CSF WCC decreased to 11 cells/μL, the low-grade fever continued. Since the defects suggested a connection to the tympanum through the tegmen tympani, cranioplasty was necessary to close the defects, in addition to tympanoplasty. On Day 56, the operation was performed. The corresponding bone defects shown on the 3D-CT images were observed (Fig. 3A). The damaged dura mater protruded into the tympanum through the bone defect, and the temporal lobe could be seen behind the dura mater (Fig. 3B). The incus was seen in the defect, and it was covered by inflammatory tissue (Fig. 3C). The dura mater was repaired, and the bone defects were closed using a bone fragment made of cranial bone and a temporal muscle fascia flap. Tympanoplasty was performed subsequently. The attic cavity was filled with soft tissue for reinforcement, and the ossicles were reconstructed. No cholesteatoma was detected during the operation. After the operation, intravenous levofloxacin (500 mg every 24 hours) was added. On Day 67, the CSF WCC was 11 cells/μL. On Day 81, the CSF WCC normalized (3 cells/μL). The meningitis did not relapse after CTRX, LZD, and levofloxacin were discontinued. The patient was discharged on Day 105 with 40 dB left conductive hearing loss. He continued to be administered oral rifampicin and had no recurrence over 9 months of follow-up at the hospital.

Discussion

Recurrence and relapse are severe problems when treating BM. As in the present case, *Streptococcus pneumoniae* is the most common pathogen associated with recurrent BM. The risk factors for recurrent BM caused by *Streptococcus pneumoniae* are head injury, congenital craniopathy, cephalocele, inner ear malformation, asplenia, IgG subclass deficiency, complement system dysfunction, HIV infection, and chronic otitis media/mastoiditis (1). Thus, it is necessary to examine the anatomical, immunological, and otolaryngeal causes.

Before the era of antibiotics, the intracranial complication of mastoiditis occurred in about 6% of cases, with a mortality rate of 71.5% in 1935 (3). After the introduction of antibiotics, the intracranial complication and mortality rates decreased to 0.36% and 18.4%, respectively, in 1995 (4). The pathophysiological mechanism of otolaryngeal infections involving the central nervous system (CNS) is considered to

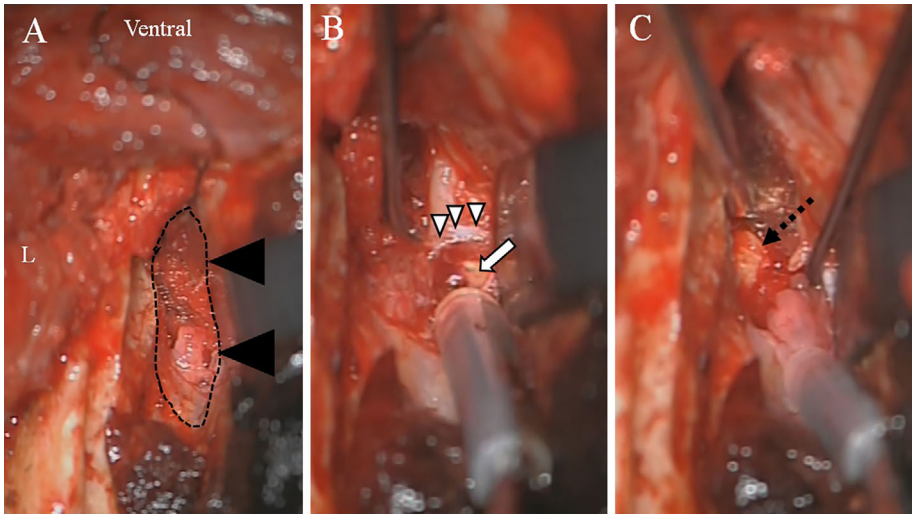

Figure 3. **A, B, C: The intraoperative findings on cranioplasty (looking down on the skull base from above) show the temporal lobe (white arrow) behind the damaged dura mater (white arrowheads). Two petrous bone defects corresponding to those seen on the 3D-CT image (black arrowhead and black-striped line) are visible. The incus is seen in the defect (black-striped arrow).**

be the osteitic destruction of the bone and dura mater, hematogenous spread by the network of the dura mater and venous sinuses, direct bacterial spread by bone fracture or otogenic intervention (5), or anatomical malformation, such as Mondini dysplasia (6). CT enables the detection of otolaryngeal infections involving the CNS, such as epidural abscess, subdural empyema, perisinus abscess, subperiosteal abscess, or sigmoid sinus thrombosis. Migirov et al. compared the CT and surgical findings of acute otitis media, and CT revealed these complications with a sensitivity of 97% (7).

However, although bone erosion is often detected, reports of bone defects are limited. In 1990, Beaumont reported a case of a 29-year-old woman with recurrent BM related to a petrous bone defect. Her bone defect and cephalocele were at the tegmen part of the petrous bone and were occluded with temporal muscle fascia, as in the present case. Axial and coronal 2-dimensional CT was used to investigate the bone defect (8).

The introduction in 1998 of MD-CT by major CT vendors has resulted in faster scan speeds, wider-range scanning, and higher z-axis spatial resolution than with traditional CT scanners. In recent years, MD-CT equipped with a larger number of detectors (64 or more) has proven capable of producing isotropic spatial resolution in a shorter scanning time, which can provide a detailed 3D multi-view image of the inner ear or cranial bone. Motojima et al. reported a case of a 6-year-old girl with recurrent BM and bone defects at the petrous apex on 3D-CT imaging (9). In the present case, the bone defect was seen at the tegmen part of the petrous bone on 3D-CT. The 3D-CT findings and intraoperative findings were similar, suggesting that 3D-CT is useful for detecting bone defects at the tegmen part, as at the petrous apex, and for investigating the minute bone structures of the skull base and simulating the intracranial operations.

Moore reported 10 cases of petrous apex cephaloceles (PACs). All of the PACs were observed along the posterolateral portion of Meckel's cave (10). Jeevan reported 32 cases of bone defects in the tegmen part, and 14 of these cases had associated chronic otitis media. A congenital temporal bone defect was reported in 6% (2 of 32 cases) (11). These reports have suggested a relationship between cephaloceles at the petrous part and Meckel's cave and between cephaloceles at the tegmen part and otitis media.

In the present case, there was bilateral thinning of the petrous bones, a cephalocele at the left side, left otitis media, and mastoiditis. The patient had no history of head trauma or intracranial intervention, nor was there any evidence of bacteremia, thrombosis, cholesteatoma, otorrhea, or inner ear malformation. The pathophysiological mechanism in the present case was thought to be related to the congenitally thin bilateral petrous bone and inflammation of the left middle ear that destroyed the tegmen tympani and neighboring dura mater, inducing a cephalocele and a relapse of BM.

In conclusion, skull bone structural abnormalities should be considered as potential causes when encountering a patient with a relapse of BM. 3D-CT is useful for detecting key features of the causal minimal bone defects and for presurgical mapping for successful treatment.

The authors state that they have no Conflict of Interest (COI).

References

1. Janocha-Litwin J, Simon K. Recurrent meningitis: a review of current literature. Przeglad epidemiologiczny **67**: 41-45, 2013.
2. Katada K. Recent development of computed tomography in Neuroradiology: Significance of multislice CT. Dansoeizo Kennkyuukai Zasshi (The Journal of the Japanese Association of

Tomography) **28**: 203-209, 2001 (in Japanese, Abstract in English).
3. Kafka MM. Mortality of mastoiditis and cerebral complications with review of 3225 cases of mastoiditis with complications. Laryngoscope **45**: 790-822, 1935.
4. Kangsanarak J, Navacharoen N, Fooanant S, Ruckphaopunt K. Intracranial complications of suppurative otitis media: 13 years' experience. Am J Otol **16**: 104-109, 1995.
5. Brydoy B, Ellekjaer EF. Otogenic meningitis: a five-year study. J Laryngol Otol **86**: 871-880, 1972.
6. Kudoh F, Sasamura Y, Udagawa Y, Iida Y, Sugita Y, Yaku Y. Bilateral Mondini dysplasia associated with recurrent meningitis. Otology Japan **7**: 207-212, 1997 (in Japanese, Abstract in English).
7. Migirov L. Computed tomographic versus surgical findings in complicated acute otomastoiditis. Ann Otol Rhinol Laryngol **112**: 675-677, 2003.
8. Beaumont GD, Sage MR. Encephalocoele involving the petrous bone. Neuroradiology **32**: 533-534, 1990.
9. Motojima T, Fujii K, Ishiwada N, et al. Recurrent meningitis associated with a petrous apex cephalocele. J Child Neurol **20**: 168-170, 2005.
10. Moore KR, Fischbein NJ, Harnsberger HR, et al. Petrous apex cephaloceles. AJNR Am J Neuroradiol **22**: 1867-1871, 2001.
11. Jeevan DS, Ormond DR, Kim AH, et al. Cerebrospinal fluid leaks and encephaloceles of temporal bone origin: nuances to diagnosis and management. World Neurosurg **83**: 560-566, 2015.